



Geochemical and physical properties of oils collected from several wells in the Shabwah depression, Yemen: implications of their characteristic organic matter input and maturity

Mohammed Hail Hakimi^{1,2} · Aref A. Lashin³ · Mikhail A. Varfolomeev^{2,4} · Nor Syazwani Zainal Abidin⁵ · Shadi A. Saeed² · Ameen A. Al-Muntaser^{2,4}

Received: 3 September 2021 / Accepted: 8 October 2021 / Published online: 29 November 2021

© Saudi Society for Geosciences 2021

Abstract

Four crude oil samples representing the Jurassic sandstone sequence were collected from several wells in the Shabwah depression and analyzed using conventional geochemical and physical methods. The results were used to evaluate the oil samples, focusing on the characteristics of their source rocks, including the origin of organic matter input, redox depositional conditions, and degree of thermal maturity. The observed physical results show that the examined oils are light crude oils owing to their high American Petroleum Institute (API) gravity of 35.0–40.1°. The high API gravity and aliphatic hydrocarbon fraction indicate that the examined oils were generated from mature source rocks. The biomarkers of *n*-alkane, isoprenoid, hopanoid, and steroid with the $\delta^{13}\text{C}$ isotopic compositions suggest that the oil samples were sourced from clay-rich rocks containing mixed organic matter with high contributions of marine organic matter and deposited under suboxic to relatively anoxic environmental conditions. The biomarker maturity indicators also suggest that the oil samples were generated from mature source rocks. According to the biomarker environmental indicators and $\delta^{13}\text{C}$ isotopic compositions, the oil samples are from the Late Jurassic Madbi shale source rock.

Keywords Shabwah depression · Yemen · Crude oil · Biomarker · $\delta^{13}\text{C}$ isotope · Geochemical correlation

Responsible Editor: Santanu Banerjee

✉ Mohammed Hail Hakimi
ibnalhakimi@yahoo.com

✉ Mikhail A. Varfolomeev
Varfolomeev@kpfu.ru

¹ Geology Department, Faculty of Applied Science, Taiz University, 6803 Taiz, Yemen

² Department of Petroleum Engineering, Kazan Federal University, Kazan 420008, Russia

³ Petroleum and Natural Gas Engineering Department, College of Engineering, King Saud University, P.O. Box 800, Riyadh 11421, Saudi Arabia

⁴ Department of Physical Chemistry, Kazan Federal University, Kazan 420008, Russia

⁵ Geosciences Department, Faculty of Science and Information Technology, Universiti Teknologi PETRONAS, 32610 Bandar Seri Iskandar, Perak, Malaysia

Introduction

The study area, the Shabwah depression in the central part of the Sabatayn Basin (Fig. 1A), is a promising area for hydrocarbon (HC) exploration, with minimal oilfields being exported (Fig. 1B). The oilfields in the Shabwah depression are prominent HC fields in northern Yemen and are managed by the Oil and Mineral Ministry in Yemen. Exploration has been initiated by Technoexport and American Occidental oil companies since 1983, aiming to test the source and reservoir rocks (SPT, 1994).

The Shabwah depression is composed of sedimentary rocks, including organic-rich shale intervals, belonging to the Late Jurassic Madbi and Late Jurassic-Early Cretaceous Naifa and Early Cretaceous Saar formations (Fig. 2). The source rock potentials of these clay-rich rocks and their ability to generate petroleum in different parts of the Shabwah depression have been investigated and reported recently (e.g., Hatem et al. 2016; Al-Matary et al. 2018; Hakimi et al. 2020a b). These studies indicate that Jurassic clay-rich rocks within the

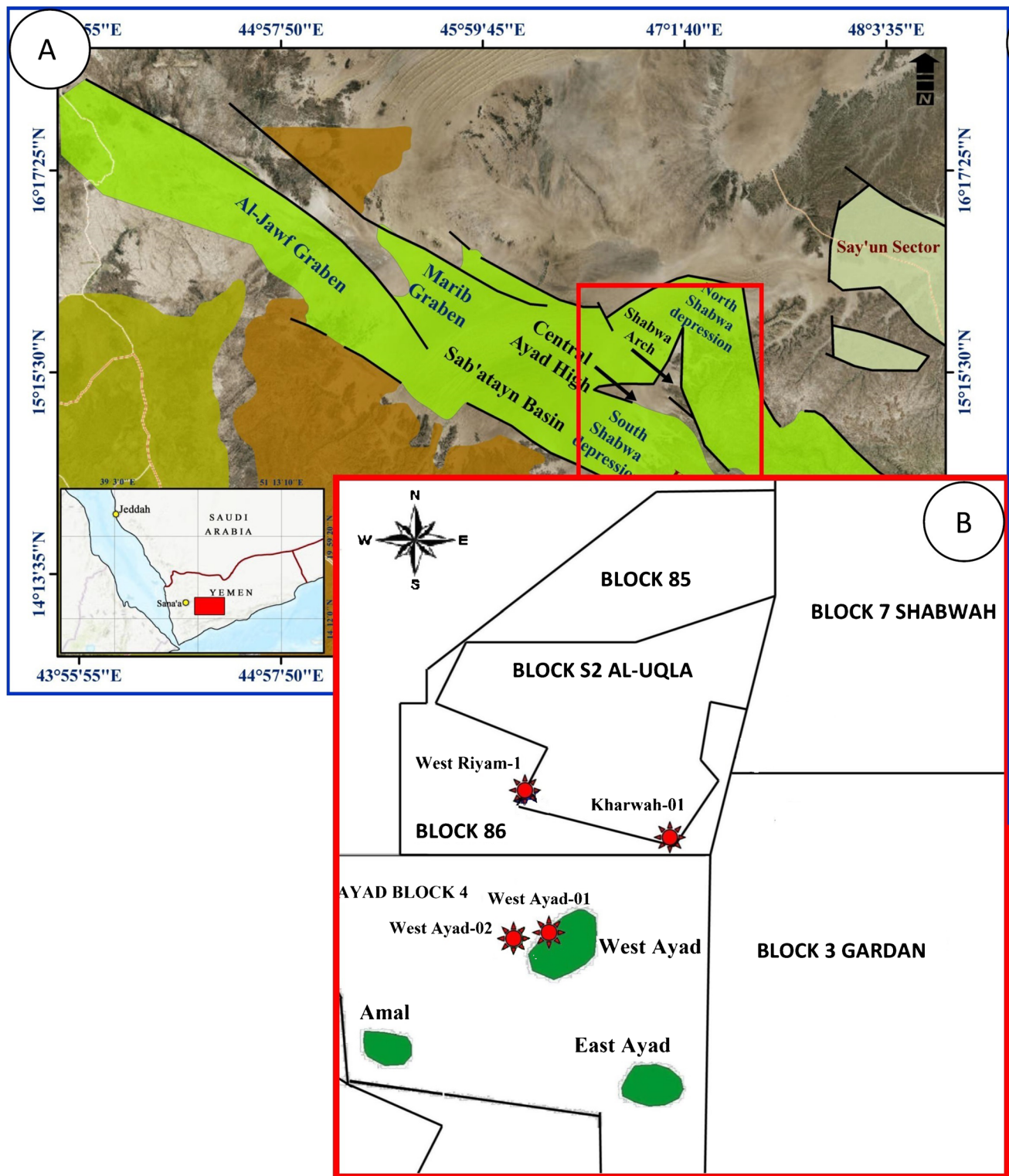


Fig. 1 A The main sub-basins (e.g., Al-Jawf, Marib, and Hajar) and the Shabwah depression in the Sabatayn rift system basin, Yemen and **B** Location map of exploration blocks in the Shabwah depression, including the studied wells

Late Jurassic Madbi and Late Jurassic-Early Cretaceous Naifa Formation were generally deposited in a marine environment setting under low-oxygen conditions. These

rocks contain mainly types II and I kerogen; thus, they are likely to be high oil-prone source rocks (e.g., Hatem et al. 2016; Hakimi et al. 2020a b). Other organic-rich shales

been investigated (e.g., Hakimi et al. 2019). However, little attention has been paid to the produced oil from wells and their characteristics, such as organic matter input, depositional environments, and degree of biodegradation and thermal maturity.

In this study, we investigated the characteristics of crude oil samples from wells in the Shabwah depression to obtain more information on the oil composition. Their kerogen forms and level of normal alterations, the origin of organic matter input, and depositional conditions of their probable source rocks are also investigated. In addition, we investigated the geochemical oil–oil and oil–source-rock correlations with their relevance to a broad perspective in exploring conventional petroleum resources. In this regard, four crude oil samples from explored wells (West Ayad-01, West Ayad-02, West Riyam-1, and Kharwah-01) in the Shabwah depression (Fig. 1B) were collected and subjected to multiple geochemical and physical analyses.

Geological setting

The Shabwah depression belongs to the Sabatayn rift system (Fig. 1A), which was associated with the Mesozoic disintegration of Gondwana during the Late Jurassic to Early Cretaceous (Redfern and Jones 1995; As-Saruri et al. 2010). The initial rifting event occurred during the end of the Jurassic and accelerated into the beginning of the Cretaceous time, followed by intermittent rifting and sagging of the basin along with sea-level incursions and withdrawals (Redfern and Jones 1995). These tectonic rifting events are manifested by several normal faults and are associated with many structural highs (horsts), lows (grabens), and tilted blocks (Fig. 3).

The Shabwah depression is filled by the Middle to Late Jurassic sedimentary sequences, followed by Cretaceous to Paleocene clastic and carbonate sediments punctuated by unconformities of different magnitudes and ages

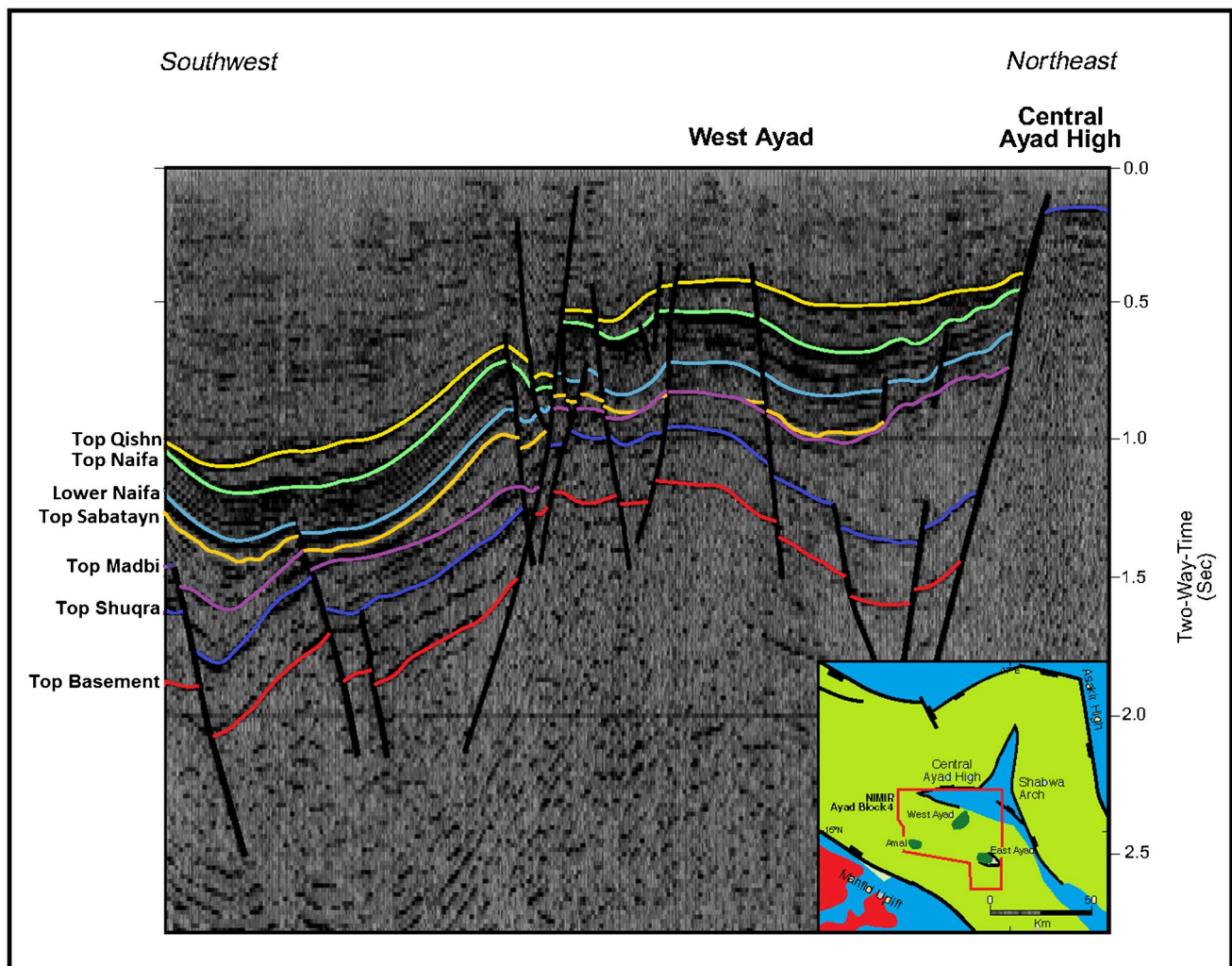


Fig. 3 Generalized stratigraphic column of Pre-Cambrian–Tertiary sequences in the Shabwah depression

(Fig. 2). These deposits are mainly related to the pre-, syn-, and post-rift tectonostratigraphic phases (Fig. 2). The pre-rift package includes the Kuhlan and Shuqra Formations with conformable contact (Fig. 2). The middle Jurassic Kuhlan Formation unconformably lies on Precambrian basement rocks (Fig. 2) and comprises continental and transgressive marine sandstones (Beydoun et al. 1998; Al-Wosabi and Al-Mashaikie 2006; Al-Hasani et al. 2018). The upper part of the Kuhlan Formation is conformably overlain by the carbonates of the Middle to Late Jurassic Shuqra Formation, which is composed of marine sediments, including limestone and calcareous shales (Fig. 2). The Shuqra Formation is, in turn, overlain unconformably by the Late Jurassic syn-rift sediment package (Fig. 2). The Madbi Formation is composed of several lithologies, including shallow marine sandstones, turbidites, and organically rich shales. It is divided into two members from base to top, namely, Meem and Lam, with a conformable contact (Fig. 2). The Madbi Formation is conformably overlain by a mixed evaporite–clastic sequence of the Late Tithonian Sabatayn Formation (Fig. 2). Mixed carbonate and shale deposits of the latest-Jurassic–earliest-Cretaceous-Naifa Formation succeed the Sabatayn Formation with a conformable contact (Fig. 2). The Naifa Formation, along with the unconformably overlying post-rift package of carbonate and clastic sedimentary rocks, ranging from Cretaceous to Paleocene in age (upper Naifa, Saar, Qishn, Fartaq/Harshiyat, Mukalla, and Umm Er Radhuma Formations), is shown in Fig. 2.

Samples and geochemical methods

Four oil samples were collected from sandstone reservoir rocks of the Middle to Late Jurassic Sabatayn and Kuhlan Formations. The samples were collected from four exploration wells (West Ayad-01, West Ayad-02, West Riyam-1, and Kharwah-01) in the Shabwah depression (Fig. 1B).

For American Petroleum Institute (API) gravity analysis, approximately 5 ml of each oil sample was analyzed using a hydrometer. This analysis was conducted at Simon Petroleum Technology Limited Laboratories, UK, and the results are made available through the Petroleum Exploration and Production Authority (PEPA) of the Republic of Yemen.

The oil samples were subsequently subjected to fractionation processes, and the bulk compositions, including aliphatic, aromatic, and polar components, were determined by the liquid column chromatography separation using different polarity solvents. Gas chromatography (GC) was performed on the aliphatic fractions of the four oil samples using an AMS-92 column, with a temperature ranging from 70 to 270 °C at a rate of 3 °C/min and a holding time of 20 min at 290 °C.

Among the samples, the aliphatic HC fraction was subjected to gas chromatography–mass spectroscopy (GC–MS) analysis. GC–MS analysis was performed using a Finnegan 4000 mass spectrometer with a gas chromatograph attached directly to the ion source with a temperature range of 60 °C to 300 °C at a rate of 3 °C/min and a holding time of 20 min at 300 °C. GC–MS analysis was employed to assess the biological marks of organisms in the saturated and aromatic HC fractions using specific ions, such as m/z 191 and 217 mass fragmentograms. The peak assignments of the specific ions were identified by comparing the retention times and mass spectra of the monitored ions with those of previous studies (Philp 1985; Peters and Moldowan 1993; Hakimi et al. 2012; Makeen et al. 2015).

In addition to GC and GC–MS analyses, the bulk $\delta^{13}\text{C}$ composition in the aliphatic and aromatic fractions of the examined oil samples was measured. Bulk $\delta^{13}\text{C}$ of the aliphatic and aromatic HC fractions was measured using a VG 602 stable isotope mass spectrometer following the standard procedure of the Simon Petroleum Technology Limited Laboratories, UK. The $^{13}\text{C}/^{12}\text{C}$ isotope ratio of CO_2 from a sample was compared with a corresponding reference (NBS22 standard), calibrated against the PDB standard.

Results and discussion

Bulk composition

The bulk compositions of the oil samples were fractionated into saturates, aromatics, and polar (NSO) components, and their relative proportions were measured (Table 1). The distributions of the oil compositions show that the oils are dominated by a saturated fraction, with a volume fraction of 39.00–60.50%. Significant amounts of aromatic HC are also present in the range of 30.90–51.50% volume; only one sample has a lower aromatic component of 11.49% volume (Table 1). The examined oil samples also have relatively small polar components (NSO) in the range of 8.60–38.76% volume (Table 1). Three oil samples have low NSO components in the range of 8.60–13.10% volume, and the other sample has the highest NSO of 38.76% (Table 1). The highest NSO of this oil sample suggests that the oil is less mature than the other three samples with low NSO content because the NSO decreases with thermal maturity. The relative percentages of the oil composition for the samples are plotted in a ternary diagram of Tissot and Welte (1984), and it suggests that the oil samples are paraffinic oils (Fig. 4).

API gravity data

Specific gravity provides genetic information and classifies crude oils. Herein, the API gravity was calculated using the

Table 1 Bulk physical and geochemical results together with carbon isotope ($\delta^{13}\text{C}$) of the oil samples from the selected wells in the Shabwah depression, NW Yemen

Blocks	Wells	Lithology	Depth (m)	Formation	API gravity	Fractions of oil compositions (wt. %)			$\delta^{13}\text{C}$ isotope compositions (‰)		
						Sat	Aro	HC	NSO non-HC	Aliphatic	Aromatic
BLOCK 4 (AYAD)	West Ayad-01	Sandstone	1330	Sabatayn	35.0	41.30	45.60	86.9	13.10	-27.60	-28.20
	West Ayad-02	Sandstone	1500		37.0	39.00	51.50	90.5	9.50	-28.20	-28.80
BLOCK S2 (AL-UQLA)	West Riyam-1	Sandstone	1755		38.0	49.75	11.49	61.24	38.76	-28.02	-27.16
	Kharwah-01	Sandstone	2752	Kuhlan	40.1	60.50	30.90	91.40	8.60	-28.10	-26.40

Sat., saturated hydrocarbons; Aro., aromatic hydrocarbons; NSO, nitrogen, sulfur, oxygen components; HC, hydrocarbon fractions (saturated + aromatic); NON-HC, non-hydrocarbon fractions (NSO)

following equation: $\text{API} = (141.5/\text{SG}) - 131.5$, where SG is the specific gravity. The oil samples have a high API gravity of 35.0–41.1° (Table 1), suggesting that they are light crude oils. The high API gravity further suggests that the oils were generated from mature source rocks because API gravity increases with an increase in the degree of thermal maturity. Further, the relationship between the depth and API gravity of the oil samples was examined. Variations in the range of API gravity were affected by the thermal gradient distributions with the burial depth, as shown by a good correlation with a high R^2 value of 0.87 (Fig. 5). The API gravity increased with an increase in burial depths due to the maturation distributions with depth.

Bulk $\delta^{13}\text{C}$ compositions

Bulk stable $\delta^{13}\text{C}$ analysis was performed on the derivative aliphatic and aromatic HC fractions of the oil samples, and it showed that the bulk $\delta^{13}\text{C}$ of the saturated and aromatic portions of the oil samples ranges from -27.60 to -28.20‰ and -26.40 to -28.80‰, respectively (Table 1). $\delta^{13}\text{C}$ values are commonly used to categorize crude oils and distinguish between the proportions of terrigenous and marine organic matter inputs in their possible source rocks (Collister and Wavrek 1996; Summons et al. 1992; Boreham et al. 2001; Sofer 1984). Accordingly, the oil samples were derived from marine organic matter, as demonstrated by the Sofer diagram of the saturated ($\delta^{13}\text{C}_{\text{Sat.}}$) and aromatic ($\delta^{13}\text{C}_{\text{Aro.}}$) isotopic compositions (Fig. 6).

In addition, $\delta^{13}\text{C}$ fraction data provide information about the deposition age of probable source rocks. $\delta^{13}\text{C}$ of the aliphatic fraction of oils is used to estimate the geologic time of their source rock during deposition (Andrusevich et al. 1998). According to Andrusevich et al. (1998), the probable source rock of the oil samples was deposited during the Jurassic to Paleogene time, as indicated by their $\delta^{13}\text{C}_{\text{Sat.}}$ values of -27.60 to -28.20‰ (Table 1). The $\delta^{13}\text{C}_{\text{Sat.}}$ and $\delta^{13}\text{C}_{\text{Aro.}}$ isotopic compositions of the Late Jurassic Madbi source rock were plotted on a Sofer diagram, and it shows that the $\delta^{13}\text{C}$ values of the oil samples are similar to those of the organic-matter-rich shale intervals of the Late Jurassic source rock (Fig. 6).

Biomarker characteristics and their interpretation to organic matter input and environmental conditions

Data interpretation from the molecular composition of the organic matter, in particular, the normal alkanes, isoprenoids, terpanes, steranes, and their ratios and parameters can complement each other in interpreting the organic matter and its depositional environmental conditions (Peters and

Fig. 4 Ternary plot of saturated and aromatic hydrocarbon fractions with polar components obtained from the examined oils, indicating that the oil samples are primarily paraffinic oils (modified after Tissot and Welte 1984)

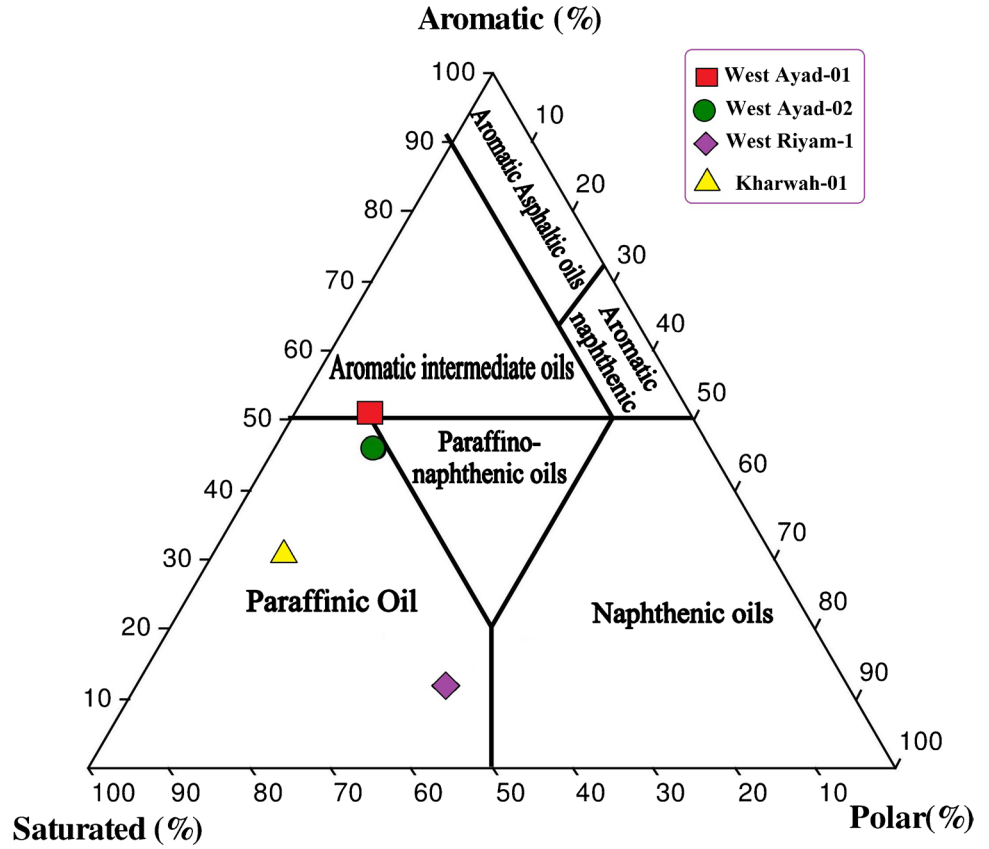
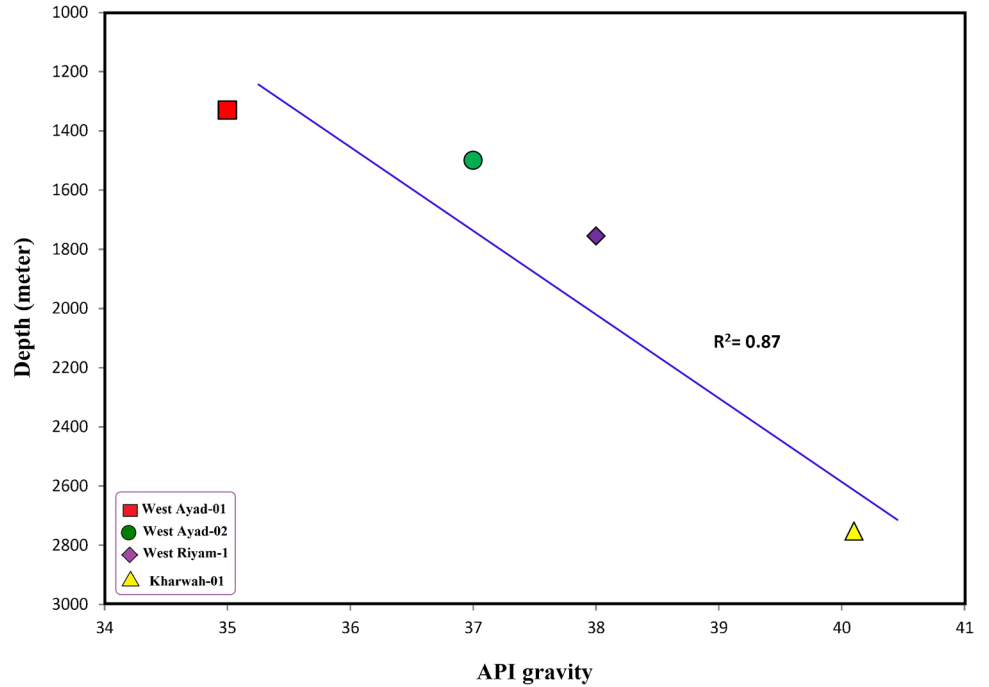


Fig. 5 Distribution of the API gravity plotted against burial depth, showing a good correlation and indicates that the API values increased with increasing burial depth



Moldowan 1993; Peters et al. 2005; Hakimi and Abdullah 2013; Snowdown et al. 2016).

The distributions of *n*-alkane and isoprenoid of the oil samples were obtained from the GC chromatograms

(Fig. 7A), and their ratios and parameters are listed in Table 2. HC in the oil samples showed a unimodal distribution with a full range of normal alkane compounds between C₁₂ and C₃₅ and acyclic isoprenoids of pristane and phytane

Fig. 6 Sofer plot of $\delta^{13}\text{C}_{\text{aro}}$ versus $\delta^{13}\text{C}_{\text{sat}}$ for the examined oil samples and extracted Madbi shale samples from Shabwah depression. The dotted line represents the best fit separation for waxy and non-waxy oils and is described by the equation $\delta^{13}\text{C}_{\text{aro}} = 1.14 \delta^{13}\text{C}_{\text{sat}} + 5.46$ (Sofer 1984)

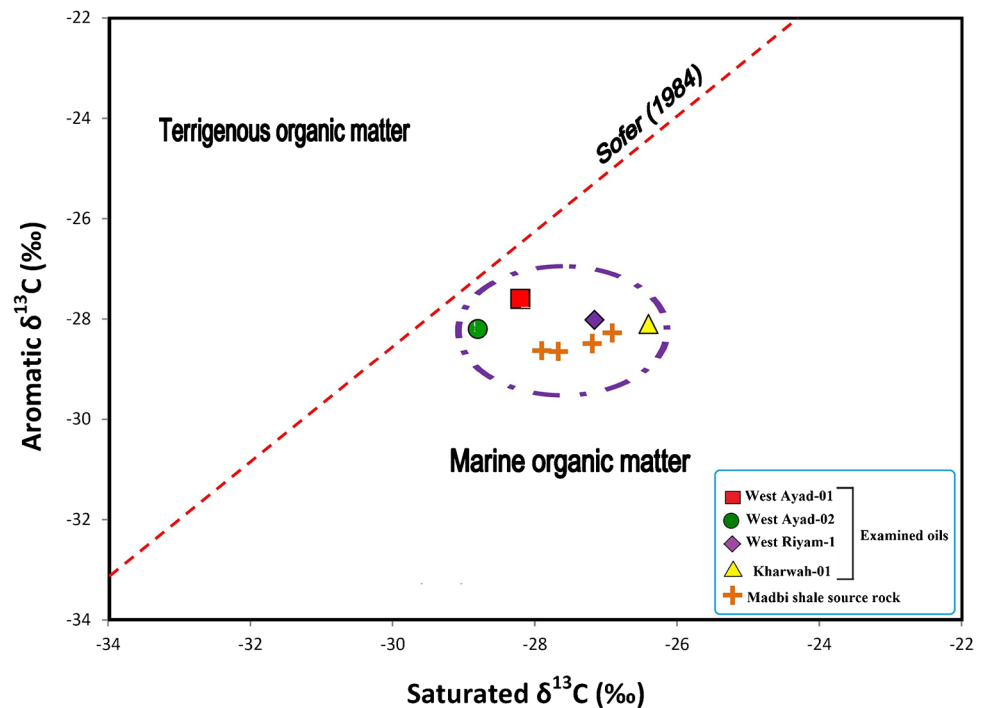


(Fig. 7A), suggesting that the oils are from source rocks containing high marine organisms and some terrestrial organic matter inputs (Cranwell 1977; Gelpi et al. 1970; Brassell et al. 1978; Eglinton and Hamilton 1967). Moreover, the interference of the organic matter input is in line with the carbon preference index (CPI) (Peters et al. 2005). CPI of most oil samples ranges between 0.84 and 1.02 (Table 2), indicating a high contribution of marine organic matter input.

The degree of waxiness was also determined using the following equation: waxiness degree = $\Sigma(n\text{-C}_{21}\text{-}n\text{-C}_{31})/\Sigma(n\text{-C}_{15}\text{-}n\text{-C}_{20})$. The waxiness of the oil samples is (0.87–2.50), further suggesting the presence of marine organic matter, as the relative abundance of waxiness level is typically indicative of organic matter derived from land plants (Connan and Cassou 1980; Johns 1986).

In addition to *n*-alkanes, the chromatograms of the oil samples are distinguished by a significant amount of acyclic isoprenoid HCs, i.e., pristane (Pr) and phytane (Ph) (Fig. 7A). Pr is greater than Ph, with a Pr/Ph ratio of 1.03–1.40 (Table 2). The isoprenoid ratio provides information about the paleodepositional environment as an indicator of redox conditions and organic matter input (Didyk et al. 1978; Haven et al. 1987; Chandra et al. 1994; Peters et al. 2005; Tserolas et al. 2019; Yi et al. 2020). The Pr/Ph ratio of the oil samples (1.03–1.40) indicates that the source rocks for the oils were deposited in transitional environments and preserved under suboxic to relatively anoxic depositional conditions. Isoprenoid ratios relative to *n*-alkane concentrations ($\text{C}_{17}\text{-C}_{18}$) were also measured as $\text{Pr}/n\text{-C}_{17}$ and $\text{Ph}/n\text{-C}_{18}$

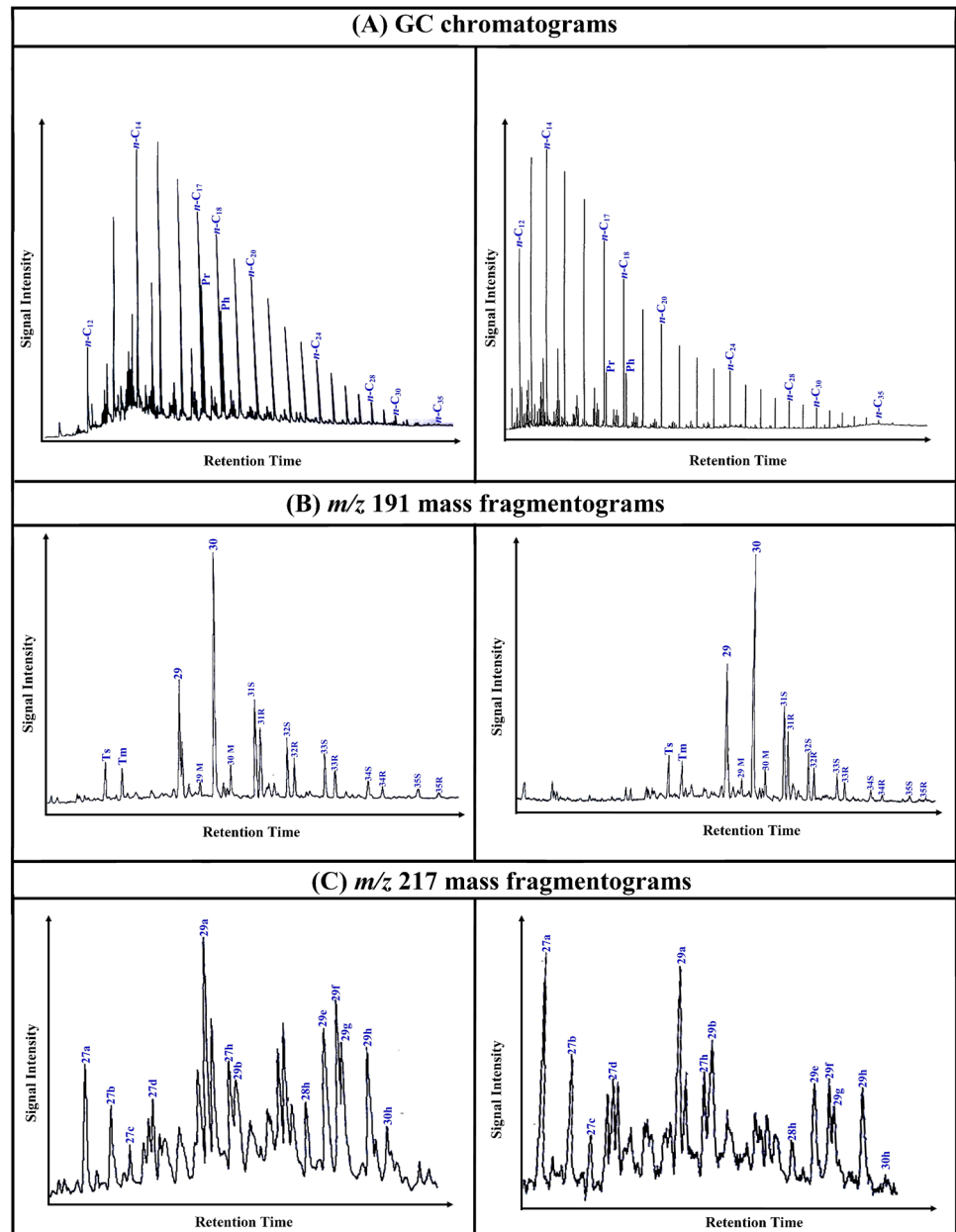
ratios, and they are in the range of 0.55–0.78 and 0.56–0.64, respectively (Table 2). These isoprenoid ratios further suggest that the oil samples were obtained from source rocks containing a mixture of organic matter, with high contributions of marine organic matter (Fig. 8A), and deposited in transitional environments under suboxic to relatively anoxic conditions (Fig. 8B). The isoprenoid Pr/Ph ratio, CPI parameter, and waxiness degree support the high contribution of marine organisms and some amount of terrestrial organic matter input in the source rocks (Fig. 9).

The biomarkers of hopanoid and steroid compounds were also present in the saturated HC fraction of the oils samples. They were obtained from *m/z* 191 and 217 mass fragmentograms (Figs. 7B and C).

The mass fragmentograms of *m/z* 191 for the oil samples show a large amount of hopanes compared to tricyclic terpanes (Fig. 7B), which are dominated by C_{30} hopane, C_{29} norhopane, and homohopanes of $\text{C}_{31}\text{-C}_{35}$, respectively (Fig. 7B). The high abundance of C_{30} hopane compared to C_{29} norhopanes in the oil samples resulted in low $\text{C}_{29}/\text{C}_{30}$ hopane values of less than 1, suggesting that the oils were generated from clay-rich source rocks (Gürgey 1999). The homohopanes of $\text{C}_{31}\text{-C}_{35}$ from the oil samples are dominated by C_{31} and decline to C_{35} homohopanes (Fig. 7B).

The 17α (H)-trisorneohopane (Tm) and 18α (H)-trisorneohopane (Ts) are important biomarkers and further used to provide information on both organic matter input and facies and maturity (Moldowan et al. 1985; Alias et al. 2012; Sarki Yandoka et al. 2015). The relative abundance of Tm is indicative of organic matter derived from land plants

Fig. 7 Gas chromatograms, m/z 191 and 217 mass fragmentograms of the saturated hydrocarbon fraction for representative two oils



(e.g., Alias et al. 2012; Sarki Yandoka et al. 2015). In this regard, the higher proportion of Ts than Tm in the m/z 191 mass fragmentogram of the analyzed sample is observed (Fig. 7B) and suggests the presence of marine organic matter with little amounts of plant input (Alias et al. 2012; Sarki Yandoka et al. 2015).

Furthermore, the steroid compounds derived from the m/z 217 mass fragmentogram are important biomarkers that provide information about the organic matter input (Huang and Meinschein 1979; Schwark and Empt 2006). The m/z 217 mass fragmentograms of the oil samples show the comparative abundance of standard regular steranes of C_{27} – C_{29} , which are characterized by a high amount of

C_{29} and C_{27} regular steranes relative to C_{28} regular sterane (Fig. 7C). The relative proportion of C_{29} , C_{27} , and C_{28} regular steranes was estimated to be 43.5–46.7%, 32.1–37.7%, and 14.2–22.2%, respectively (Table 2). These distributions of C_{27} – C_{29} regular steranes suggest high contributions of planktonic-bacterial organic matter, as demonstrated by the ternary diagram of regular steranes (Fig. 10). Further, the dominance of the C_{27} and C_{29} regular steranes in the analyzed oil samples is a good indicator of the presence of red and green algae during the accumulation of the source rock (Schwark and Empt 2006). The C_{27}/C_{29} and Pr/Ph ratios further suggest a mixed organic matter with a high contribution of marine organic matter

Table 2 Selected Biomarker parameters of the oil samples from the studied wells in the Shabwah depression, NW Yemen, illustrating source organic matter, depositional environmental conditions, and thermal maturity indicators

Wells	Depth (m)	Biomarker indicators of the environmental conditions and organic matter input							Biomarker indicators of the thermal maturity							
		Pr/Ph	Pr/C ₁₇	Ph/C ₁₈	WI	CPI	Regular steranes (%)	C ₂₇ /C ₂₉ regular sterane	C ₂₉ /C ₃₀	C ₃₂ 22S/ (22S + 22R)	MC ₃₀ /HC ₃₀	Ts/Tm	C ₂₉ 20S/20S + 20R	C ₂₉ ββ/(ββ+αα)		
							C ₂₇	C ₂₈	C ₂₉							
West Ayad-01	1330	1.00	0.29	0.36	0.46	0.99	49.8	10.5	39.7	1.25	0.69	0.57	0.12	1.01	0.47	0.60
West Ayad-02	1500	1.25	0.45	0.30	0.48	0.96	53.5	11.5	35.0	1.53	0.55	0.58	0.14	1.41	0.45	0.63
West Riyam-1	1755	1.26	0.64	0.56	0.43	1.00	41.7	18.1	40.2	1.04	0.62	0.58	0.11	1.20	0.56	0.58
Kharwah-01	2752	1.40	0.78	0.56	0.45	1.04	39.0	20.1	40.9	0.95	0.65	0.62	0.09	1.16	0.58	0.55

Pr; pristane; Ts, (C₂₇ 18α(H)-22,29,30-trisnorhopane); CPI, Carbon preference index: $\{2(C_{23} + C_{25} + C_{27} + C_{29}) / (C_{22} + 2[C_{24} + C_{26} + C_{28}] + C_{30})\}$; Ph, Phytane; Tm, (C₂₇ 17α(H)-22,29,30-trisnorhopane); WI, Waxiness degree: $\sum(n-C_{21}-n-C_{31}) / \sum(n-C_{15}-n-C_{20})$; C₃₀M/C₃₀H, C₃₀ moretane/C₃₀ hopane; C₂₉/C₃₀, C₂₉ norhopane/C₃₀ hopane

accumulated under suboxic to oxic environmental conditions (Fig. 11).

Oil characteristics and their relevance to biodegradation and maturity

The exploration of oil samples is affected by the high costs of refining biodegraded oils (Jones et al. 2008). Therefore, there is a need to study the biodegradation processes and their impact on the physical properties and chemical compositions of fresh oils. Regarding physical properties, biodegraded oils have lower API gravity and higher viscosity than fresh oils (Barth et al. 2004; Luo and Gu 2005 and Luo and Gu 2007). However, oils containing heavy asphaltic materials are generally more degraded than oils rich in saturated and aromatic HCs (Connan 1984; Larter et al. 2005; Larter et al. 2003; Al-Khafaji et al. 2020).

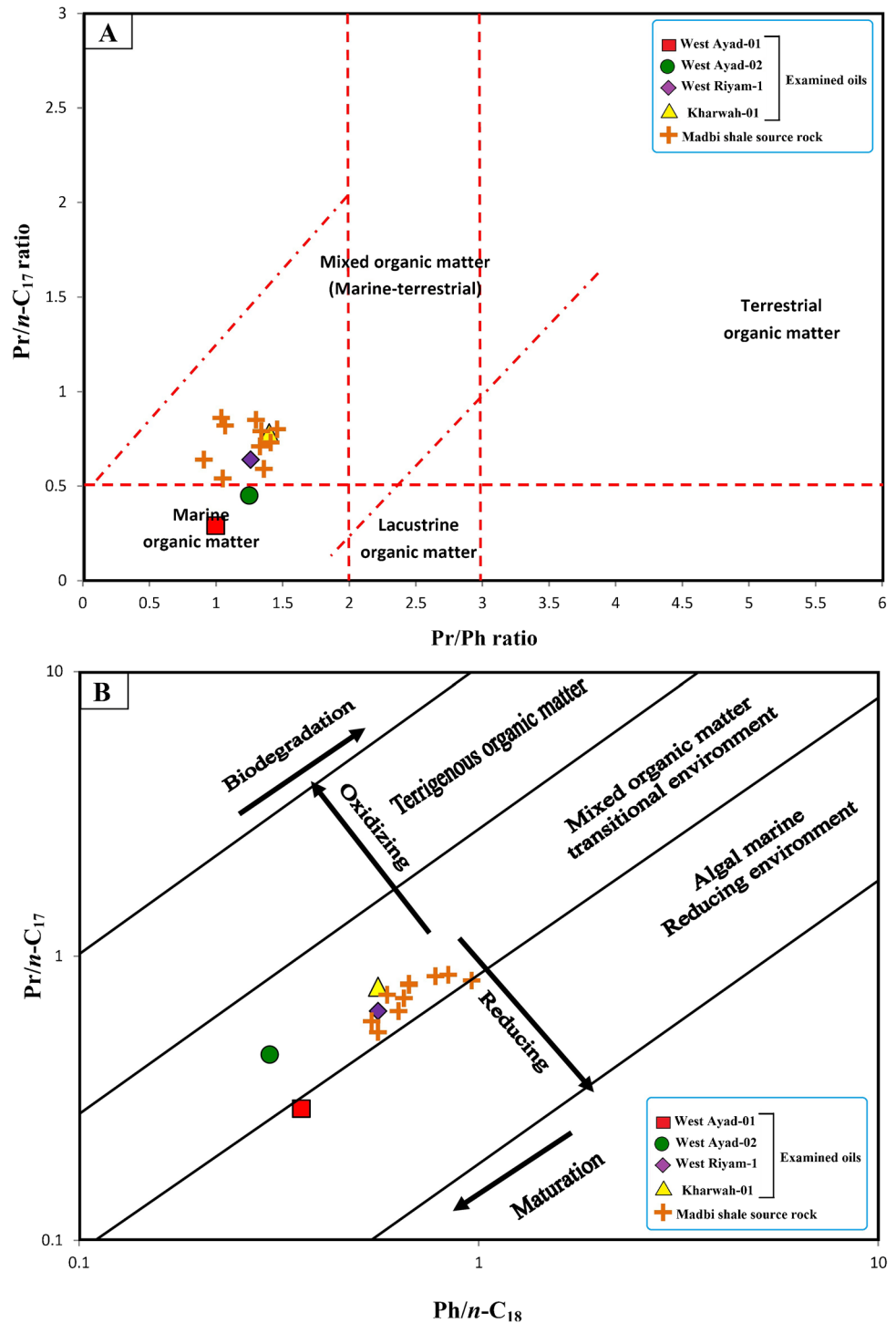
In addition to physical properties and chemical compositions, several studies have reported that the level of biodegradation is shown by the abundance and distributions of normal alkane and acyclic isoprenoids on gas chromatograms and the shape of baselines of the chromatograms (Connan 1984; Head et al. 2003; Peters et al. 2005). Light normal alkanes and acyclic isoprenoids can be removed in the early stage of biodegradation of oil, whereas heavy branched and cyclic saturated HCs and aromatics are the most resistant HCs to biodegradation (Larter et al. 2005).

Herein, the observed geochemical and physical properties of the oil samples indicate the occurrence of biodegradation. The physical properties indicate that the oil samples are not heavy but light oils, thus they were not biodegraded. The relatively high API gravity of greater than 22° indicates the absence of biodegradation (Wang et al. 2021). In addition to API gravity, the high abundance of aliphatic and aromatic HCs compared with NSO compounds (Table 1) indicates the absence of biodegradation.

Furthermore, the biodegradation of the oil samples was assessed using the distribution of normal alkanes and acyclic isoprenoids (Connan 1984; Head et al. 2003; Peters et al. 2005; Larter et al. 2005). The distribution of HCs generally indicates that the oil samples were not biodegraded, which is consistent with the full complement of light and heavy n-alkanes ranges between C₁₂ and C₃₅ and isoprenoids with a straight baseline (Fig. 7A).

In addition to biodegradation, the degree of maturation for the oil samples was assessed using the oil composition and API gravity. The bulk oil composition can also be used to predict the thermal maturity of their possible source rocks (Killops et al. 1998). Relatively high content of polar components (resins and asphaltenes) indicates low maturity of source rock because polar components decrease with the thermal maturity (Killops et al. 1998; Egbo et al. 2020). Herein, the oil samples showed high HC fractions (aliphatic

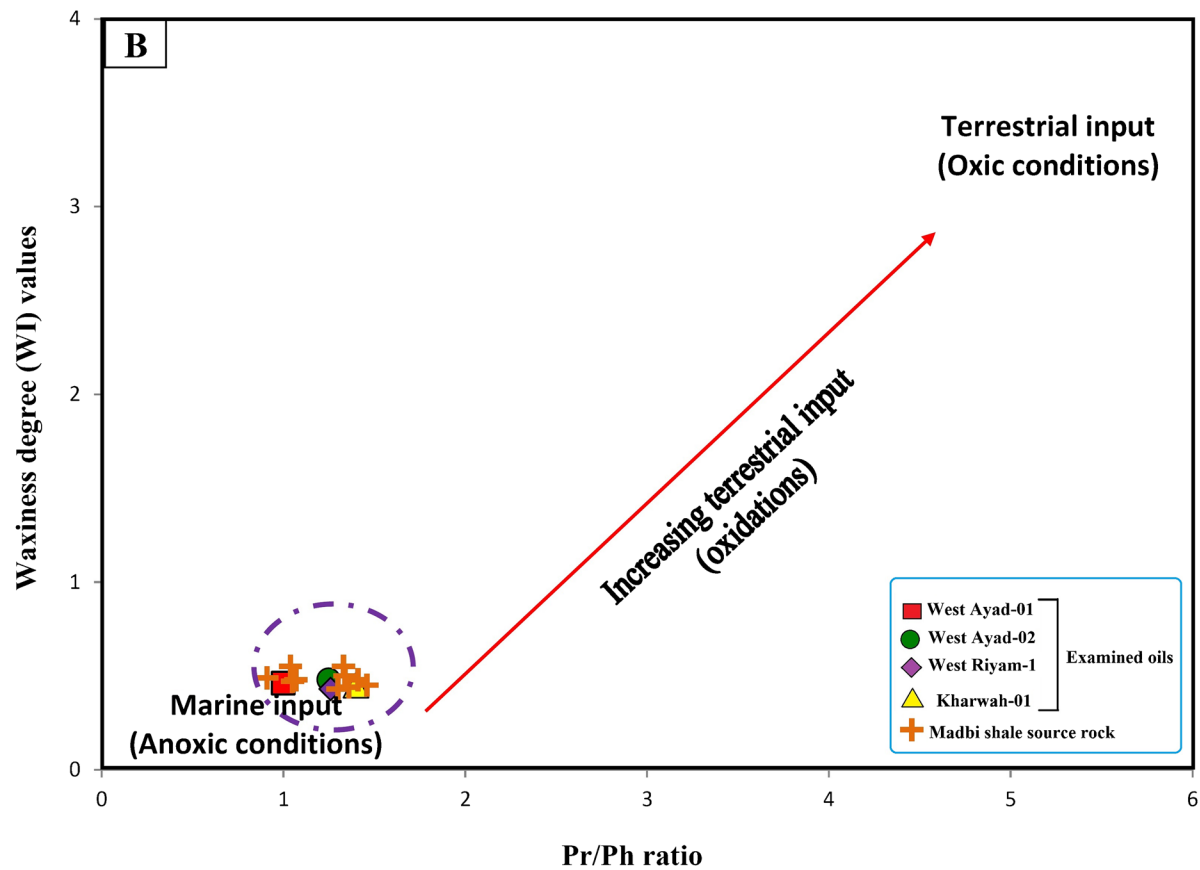
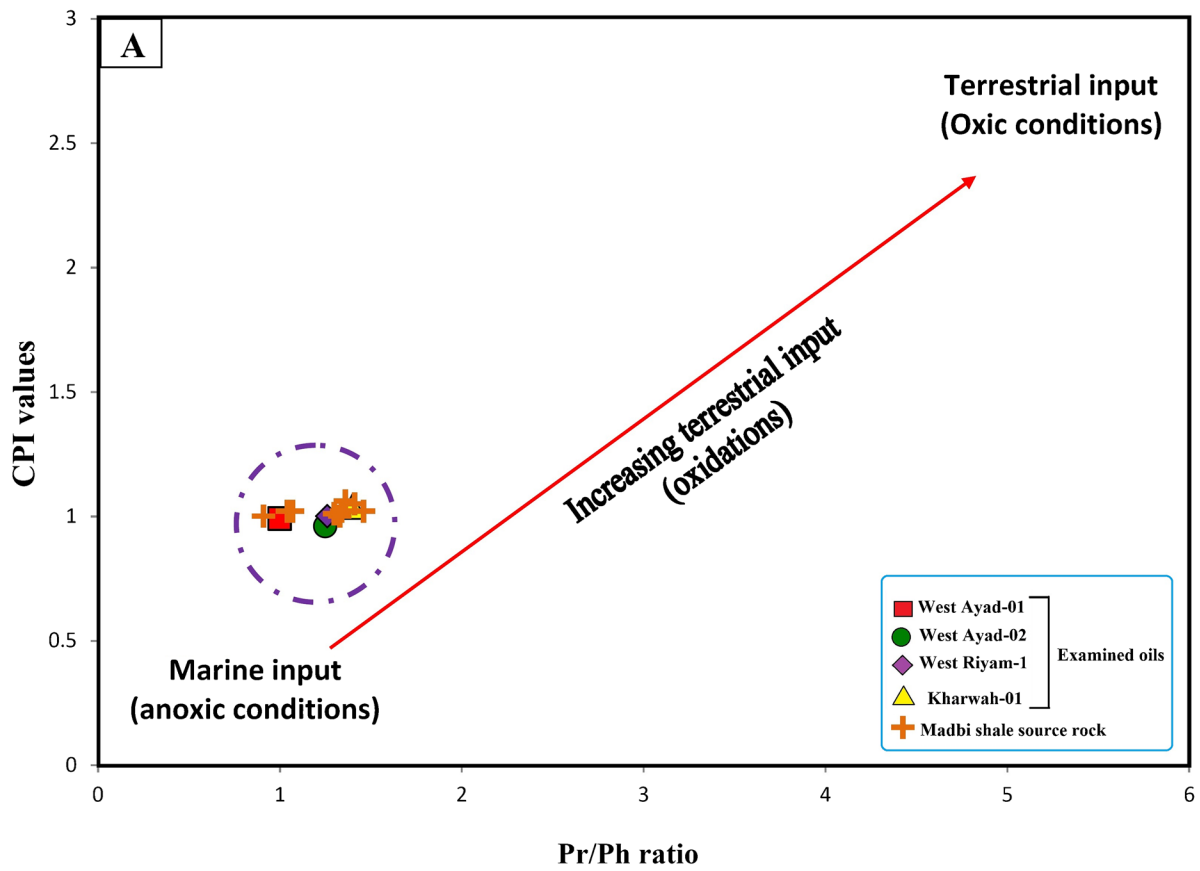
Fig. 8 Geochemical biomarker results of the examined oil samples and extracted Madbi shale samples from Shabwah depression: **a** pristane/phytane versus pristane/*n*-C₁₇ and **b** pristane/*n*-C₁₇ versus phytane/*n*-C₁₈ (from Shanmugam, 1985), indicating that the examined oils were generated from source rocks containing a mixture of organic matter



and aromatic HC) compared with other polar components, indicating that the oils were generated from a mature source rock, corresponding to the VRO values between 0.70 and 0.90%, as demonstrated by the plots of the saturate, aromatic, and polar portions on the Tissot and Welte (1984) diagram (Fig. 12). This indicates that the HC (aliphatic + aromatic) fractions increased with a decrease in NSO components due

to the thermal alteration of organic matter input the source rock (Egbo et al. 2020).

The mature stage of the probable source rock is also consistent with the API gravity (Table 1), and there is a positive correlation between saturated HCs and API gravity, with the R² value of 0.78 (Fig. 13). Therefore, the proportion of saturated HCs and API were increased with maturity.



◀ **Fig. 9** Geochemical biomarker results of the examined oil samples and extracted Madbi shale samples from Shabwah depression: **a** pristane/phytane versus CPI and **b** pristane/phytane versus waxiness degree, further indicating that the examined oils were generated from source rocks containing marine organic matter

Furthermore, the maturity biomarker, namely, the 22S/(22S + 22R) ratio of C₃₂ homohopanes, moretane to hopane (C₃₀M/C₃₀H) ratio, Ts/Tm ratio, and C₂₉ sterane the 20S/(20S + 20R) and $\beta\beta/(\beta\beta + \alpha\alpha)$ ratios, were derived from the distribution of terpanes and steranes in the *m/z* 191 and 217 mass fragmentograms (Fig. 7B and C). These biomarkers and ratios are the most reliable biomarker ratios in the analyzed oil samples and generally detect the maturity level between early mature and mature levels (Seifert and Moldowan 1978, 1981, 1986; Mackenzie et al. 1980).

The C₃₂ homohopane ratio applies to equilibrium points and reaches a maximum of 0.65 (Seifert and Moldowan 1986). Thus, the immature zone of source rocks is represented by a C₃₂ ratio of less than 0.50, and early to moderate mature source rocks have a C₃₂ ratio of 0.50–0.58. An equilibrium point of more than 0.58 indicates peak oil window and high maturity stages (Seifert and Moldowan 1986). Based on this scale, the examined oils are thermally mature and have reached moderate to peak maturity stages of the oil-generation window, with a C₃₂ hopane ratio of 0.54–0.57 (Table 2).

The thermal maturity stage of the analyzed oil samples is also demonstrated by the C₂₉ 20S/(20S + 20R) and $\beta\beta/(\beta\beta + \alpha\alpha)$ sterane ratios (Seifert and Moldowan 1978, 1981, 1986). C₂₉ 20S/(20S + 20R) and $\beta\beta/(\beta\beta + \alpha\alpha)$ sterane ratios of greater than 0.35 and 0.40, respectively, suggest a source rock in the oil window maturity level (Hakimi et al. 2012; Gharib et al. 2021). Herein, the C₂₉ 20S/(20S + 20R) and $\beta\beta/(\beta\beta + \alpha\alpha)$ sterane ratios for the oil samples are in the ranges of 0.44–0.48 and 0.50–0.53, respectively (Table 2), indicating mature source rocks (Fig. 14A). In addition, the C₃₂ hopane ratio was combined with the C₂₉ $\beta\beta/(\beta\beta + \alpha\alpha)$ sterane ratios, and the result further suggests an early to moderate mature source rock, consistent with the VR values of 0.50–0.80% (Fig. 14B).

Ts/Tm and C₃₀ moretane/C₃₀ hopane (C₃₀M/C₃₀H) ratios were also used to evaluate the thermal maturation of the source rocks (Mackenzie et al. 1980; Peters et al. 2005; Roushdy et al. 2010; Nady et al. 2014). According to Peters et al. (2005), during catagenesis, C₂₇ 18 α - trisnorhopane (Ts) is more stable than C₂₇ 17 α - trisnorhopane ratio (Tm). The mass fragmentograms of *m/z* 191 (Fig. 7B) show that the Ts/Tm ratio ranges from 0.67 to 1.99 (Table 2). These Ts/Tm and C₃₀M/C₃₀H ratios were used to evaluate the thermal maturation (Mackenzie et al. 1980). The Ts/Tm ratio and low CM30/C30 ratio of less than 0.15 for the analyzed

oil samples (Table 2) confirm mature source rocks in the range of early to peak oil window maturity (Fig. 14C).

The CPI values derived from the distribution of normal alkanes were also used to evaluate the thermal maturation of the analyzed oils and their source rocks. Although CPI is affected by source facies (Peters et al. 2005), it can be used as an indicator of thermal maturity (Bray and Evans 1961). According to Bray and Evans (1961), CPI decreases with an increase in thermal maturity, with values close to unity indicating mature source rocks (Bray and Evans 1961). Consistent with previous maturity indicators, the CPI range of the oil samples was 0.90–1.05, indicating that the oil samples were generated from mature source rocks.

Geochemical correlations (oil–oil and oil–source correlations)

The degrees of the genetic link of oils and their source rocks were demonstrated by the physical and geochemical properties of the oil in this study and a previous study by Hakimi et al. 2020a b). The lipid biomarker distributions, $\delta^{13}\text{C}$ isotopic compositions, and physical properties of the oil samples were used to assess the characteristics of the oil samples. Then, the oil–oil and oil–source rock correlations were determined. There was a positive oil–oil correlation, and the oil samples appeared to have been generated from a single source rock, as indicated by the clustering of their physical and geochemical properties (Figs. 2 and 3). The source rock is speculated to be a clay-rich facies consisting of mixed organic matter with a high accumulation of marine organic matter and deposited in a marine environment under suboxic to relatively anoxic conditions, which is consistent with the results of molecular biomarkers and $\delta^{13}\text{C}$ compositions of saturated and aromatic HC fractions. The oil samples are geochemically similar and consistent with those of the Late Jurassic Madbi shale source rock, as indicated by the clustering of their environmental biomarker indicators and $\delta^{13}\text{C}$ isotopic compositions (Fig. 5–14). The clustering of their molecular and $\delta^{13}\text{C}$ isotope results indicates a positive oil–source-rock correlation, suggesting that the oil samples were generated from the Madbi shale source rock at sufficient maturity levels.

Conclusions

In this study, we investigated the geochemical and physical properties of oil samples from several wells in the Shabwah depression and characterized source rocks, including the origin of organic matter input, redox depositional conditions, lithology, and degree of thermal maturity. Based on the obtained results, the following conclusions are drawn:

Fig. 10 Ternary diagram of regular steranes (C_{27} – C_{29}) in the examined oil samples and extracted Madbi shale samples from Shabwah depression, indicating the relationship between sterane compositions, concerning organic matter input (modified after Huang and Meinschein 1979)

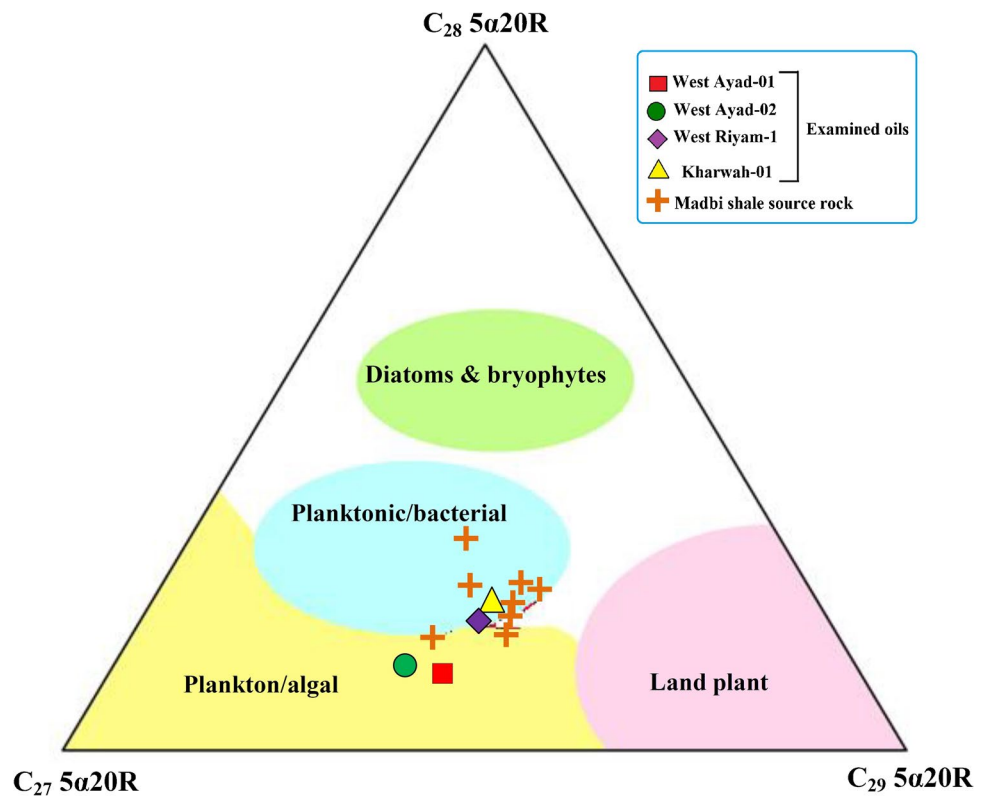
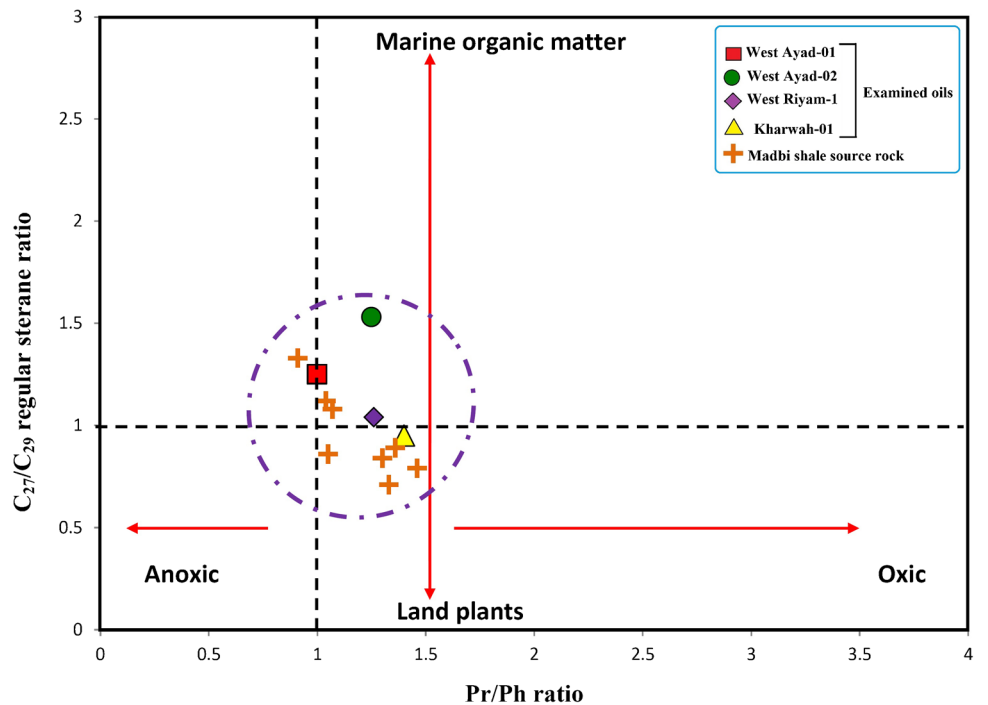


Fig. 11 Cross-plot for Pr/Ph versus the C_{27}/C_{29} regular sterane ratio of the examined oil samples and extracted Madbi shale samples from Shabwah depression, which further infers a mixed organic matter input, with high contributions of marine organic matter



1. The oil samples have a high API gravity of 35.0–40.1° and are considered light crude oils. The API gravity and high aliphatic HC indicate that the oil samples were generated from the mature source rock.
2. The oil samples were derived from a clay-rich source rock with a high content of marine planktonic/algae and terrestrial land plants and deposited under suboxic to relatively anoxic conditions. These findings are dem-

Fig. 12 Ternary diagram showing the gross composition (saturated, aromatic and polar) of the analyzed samples, suggesting mature oils (modified after Peters et al. 2005)

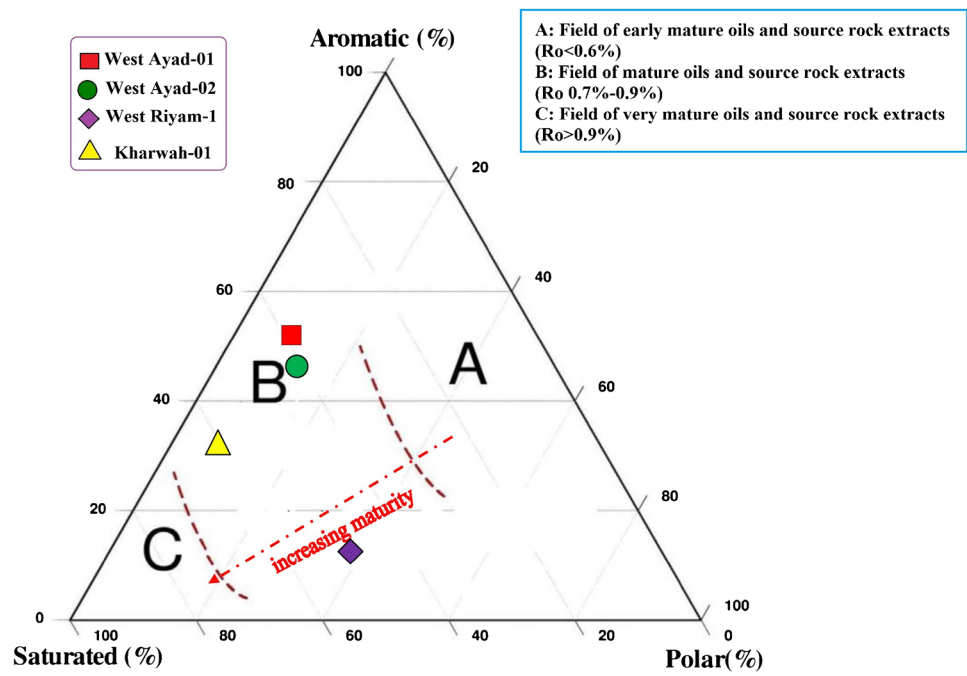
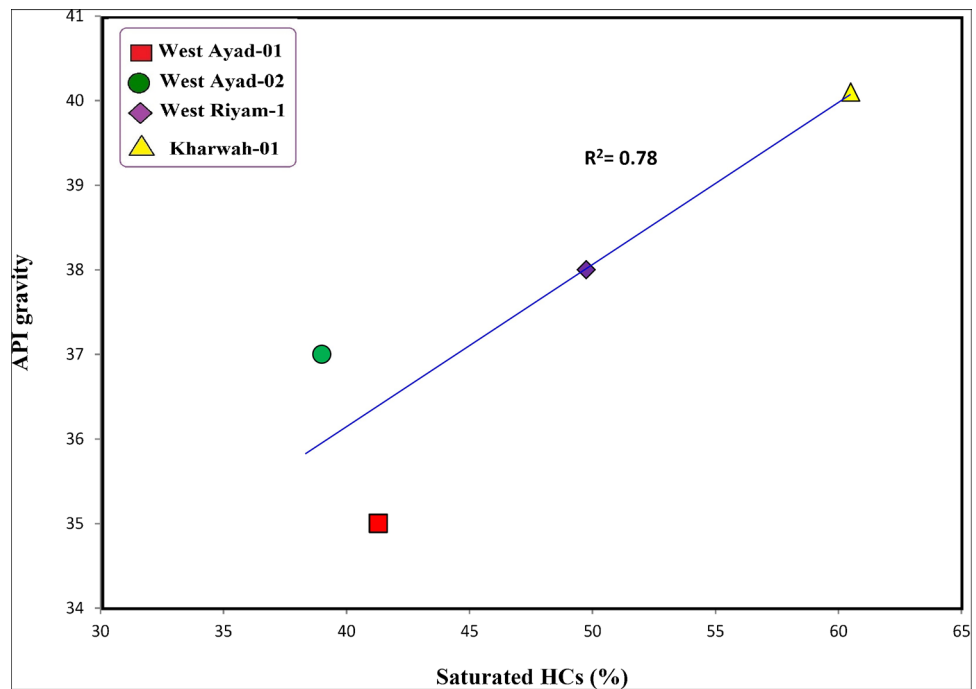


Fig. 13 Relationship between saturated fraction and API gravity, showing a good correlation and indicates that the API values increased with increasing saturated HCs

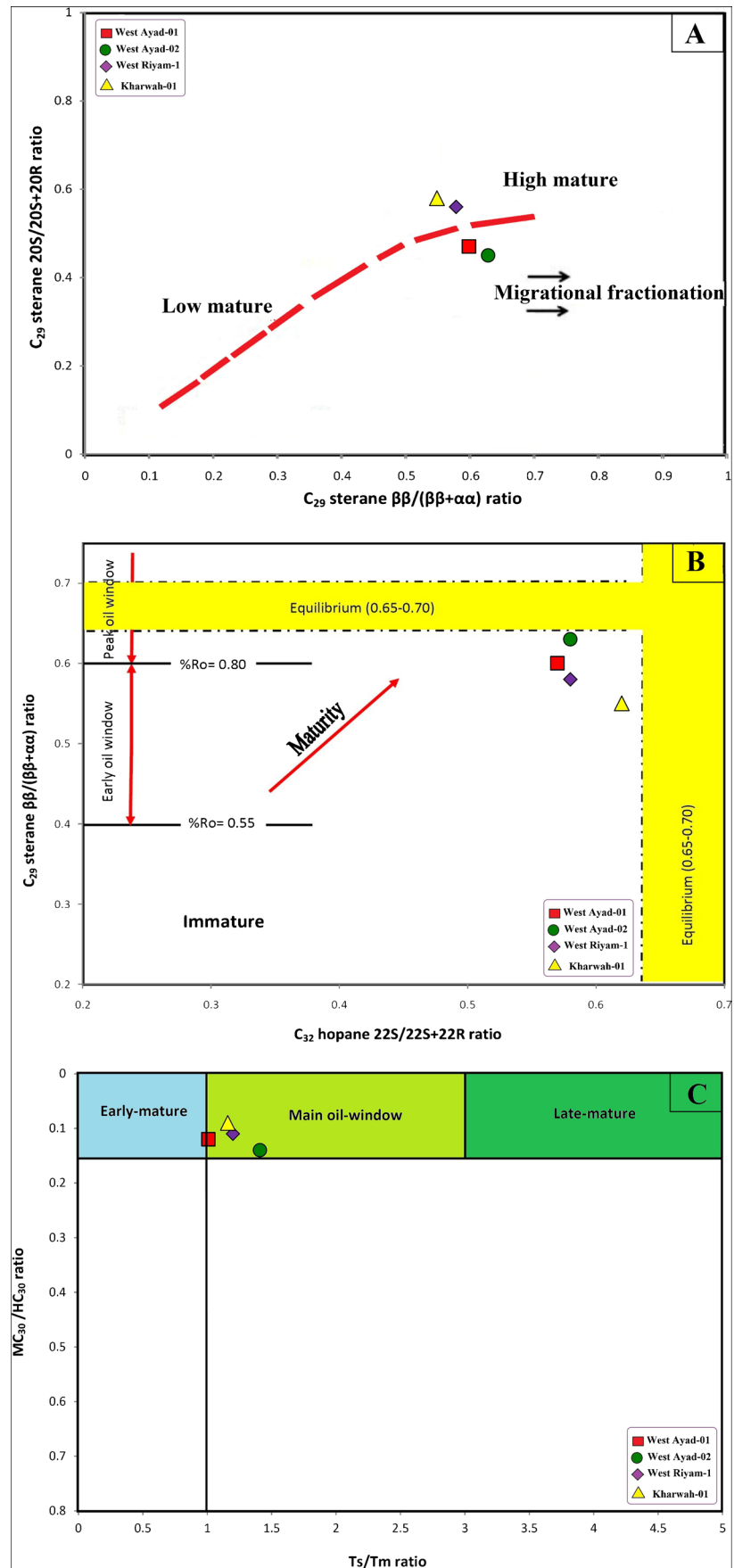


onstrated by the lipid biomarkers, in particular, the normal alkanes, isoprenoids, terpanes, and steranes together with the $\delta^{13}\text{C}$ isotopic compositions.

3. Both physical and geochemical parameters suggest that the examined oils were not altered by biodegradation and were generated from the mature source rock.

4. The oil samples are geochemically similar and consistent with those of the Madbi clay-rich source rock, as indicated by the clustering of their environmental biomarker indicators and $\delta^{13}\text{C}$ isotopic compositions.

Fig. 14 Biomarker maturity ratios of the analyzed oil samples: **A** C₂₉ sterane 20S/(20S + 20R) versus ββ/(ββ + αα), **B** C₃₂ hopane 22S/(22S + 22R) versus C₂₉ sterane ββ/(ββ + αα), and **(C)** Ts/Tm ratio versus CM₃₀/C₃₀ ratio, showing that the oils were generated from a mature source rock, ranging from a moderate to peak oil-generation window



Acknowledgements The authors acknowledge the Petroleum Exploration and Production Authority (PEPA), Republic of Yemen, for providing the geochemical data used in this research. This work also was supported by the Ministry of Science and Higher Education of the Russian Federation under agreement No. 075-15-2020-931 within the framework of the development program for a world-class Research Center “Efficient development of the global liquid hydrocarbon reserves.” The authors also extend their sincere appreciation to the Researchers Supporting Project number (RSP-2021/92), King Saud University, Riyadh, Saudi Arabia. The comments by an anonymous reviewers are also gratefully acknowledged.

Declarations

Conflict of interest The authors declare that they have no competing interests.

References

- Al-Hasani A, Hakimi MH, Saaid IM, Salim AMA, Mahat SQ, Ahmed AA, Umar AA (2018) Reservoir characteristics of the Kuhlhan sandstones from Habban oilfield in the Sabatayn Basin, Yemen and their relevance to reservoir rock quality and petroleum accumulation. *J Afr Earth Sc* 145:131–147
- Al-Khafaji AJ, Hakimi MH, El-Khedr Ibrahim EK, Najaf AA, Al Faihi H, Lashin A (2020) Organic geochemistry of oil seeps from the Abu-Jir Fault Zone in the Al-Anbar Governorate, Western Iraq: implications for early-mature sulfur-rich source rock. *J Petrol Sci Eng* 184:23–35
- Alias FL, Abdullah WH, Hakimi MH, Azhar MH, Kugler RL (2012) Organic geochemical characteristics and depositional environment of the Tertiary Tanjong Formation coals in the Pinangah area, onshore Sabah. *Malaysia Int J Coal Geol* 104:9–21
- Al-Matary AM, Hakimi MH, Al-Sofi S, Al-Nehmi YA, Al-haj MA, Al-Hmdani YA, Al-Sarhi AA (2018) Preliminary source rock evaluation and hydrocarbon generation potential of the early cretaceous subsurface shales from Shabwah sub-basin in the Sabatayn Basin, Western Yemen. *J Afr Earth Sc* 142:12–21
- Al-Wosabi MA, Al-Mashaikie, SZ (2006). Investigation of facies types and associations of Kuhlhan Red Bed Formation in NW Yemen: a new hypothesis for origin and depositional environment. *SQU J Sci* 11–38
- Andrusevich VE, Engel MH, Zumberge JE, Brothers LA (1998) Secular, episodic changes in stable carbon isotope composition of crude oils. *Chem Geol* 152:59–72
- As-Saruri MA, Sorkhabi R, Baraba R (2010) Sedimentary basins of Yemen: their tectonic development and lithostratigraphic cover. *Arab J Geosci* 3:515–527
- Barth T, Høiland S, Fotland P, Askvik KM, Pedersen BS, Borgund AE (2004) Acidic compounds in biodegraded petroleum. *Org Geochem* 35:1513–1525
- Beydoun ZR, M Al-Saruri, H El-Nakhal, IN Al-Ganad, R S Baraba, ASO Nani, MHAJ- Aawah (1998) International lexicon of stratigraphy, 2nd ed., v. 3: Republic of Yemen, International Union of Geological Sciences and Ministry of Oil and Mineral Resources Publication 34 245
- Boreham CJ, Hope JM, Hartung-Kagi B (2001) Understanding source, distribution and preservation of Australian natural gas: a geochemical perspective. *The Australian Production and Petroleum Exploration Association Journal* 41:523–547
- Brannan J, Sahota G, Gerdes KD, Berry JAL (1999) Geological evolution of the central Marib-Shabwa basin, Yemen. *GeoArabia* 4:9–34
- Brassell SC, Eglinton G, Maxwell JR et al (1978) Natural background of alkanes in the aquatic environment. In: Hutzinger O et al (eds) aquatic pollutants: transformation and biological effects: Oxford. Pergamon Press, pp 69–86
- Bray EE, Evans ED (1961) Distribution of *n*-paraffins as a clue to recognition of source beds. *Geochim Cosmochim Acta* 22:2–15
- Chandra K, Mishra CS, Samanta U, Gupta A, Mehrotra KL (1994) Correlation of different maturity parameters in the Ahmedabad-Mehsana block of the Cambay basin. *Org Geochem* 21:313–321
- Collister JW, Wavrek DA (1996) 13C compositions of saturate and aromatic fractions of lacustrine oils and bitumens: evidence for water column stratification. *Org Geochem* 24:913–920
- Connan J (1984) Biodegradation of crude oils in reservoirs. In: Brooks J, Welte DH (eds) *Advances in Petroleum Geochemistry*. Academic Press, London, pp 299–330
- Connan J, Cassou AM (1980) Properties of gases and petroleum liquids derived from terrestrial kerogen at various maturation levels. *Geochim Cosmochim Acta* 44:1–23
- Cranwell PA (1977) Organic geochemistry of Cam Loch (Sutherland) sediments. *Chem Geol* 20:205–221
- Didyk BM, Simoneit BRT, Brassell SC, Eglinton G (1978) Organic geochemical indicators of palaeoenvironmental conditions of sedimentation. *Nature* 272:216–222
- Egbo OK, Adeigbe OC, Esegbue O (2020) Preliminary geochemical investigation of some crude oils from the Niger Delta Basin Nigeria. *J Res Environ Earth Sci* 6:18–25
- Eglinton G, Hamilton RJ (1967) Leaf epicuticular waxes. *Science* 156:1322–1334
- El Nady MM, Harb FM, Mohamed NS (2014) Biomarker characteristics of crude oils from Ashrafi and GH oilfields in the Gulf of Suez, Egypt: an implication to source input and paleoenvironmental assessments. *Egypt J Pet* 23:455–459
- Gelpi E, Schneider H, Mann J, Oro J (1970) Hydrocarbons of geochemical significance in microscopic algae. *Phytochemistry* 9:603–612
- Gharib AF, Özkan AM, Hakimi MH, Zainal Abidin N, Lashin A (2021) Integrated geochemical characterization and geological modeling of organic matter-rich limestones and oils from Ajeel Oilfield in Mesopotamian Basin Northern Iraq. *Mar Pet Geol* 126:104930
- Gürgey K (1999) Geochemical characteristics and thermal maturity of oils from the Thrace Basin (western Turkey) and western Turkmenistan. *J Petrol Geol* 22:167–189
- Hakimi MH, Abdullah WH (2013) Geochemical characteristics of some crude oils from Alif Field in the Marib-Shabowah Basin, and source-related types. *Mar Pet Geol* 45:304–314
- Hakimi MH, Abdullah WH, Shalaby MR (2012) Molecular composition and organic petrographic characterization of Madbi source rocks from the Kharir Oilfield of the Masila Basin (Yemen): Palaeoenvironmental and maturity interpretation. *Arab J Geosci* 5:817–831
- Hakimi MH, Alaug AS, Alramisy GA, Ahmed AF (2019) Petroleum that has migrated into an outcropping of the Jurassic Ayad Salt Dome of Shabwah depression, Yemen. *Pet Sci Technol* 37:296–304
- Hakimi MH, Al-Matary AM, Abdullah WH, Adeep A, Lashin AA, Shah SB, Yahya AMA (2020a) Oil source rock characteristics of the pelagic carbonates in the Shabwah depression, southeastern Sabatayn Basin. *Yemen. Carbonates Evaporites* 35(2020):45. <https://doi.org/10.1007/s13146-020-00578-5>
- Hakimi MH, Al-Matary AM, El-Mahdy O, Hatem BA, Kahal AY, Lashin AA (2020b) Organic geochemistry characterization of Late Jurassic bituminous shales and their organofacies and

- oil generation potential in the Shabwah depression, southeast Sabatayn, Yemen. *J Pet Sci Eng* 188:106951
- Hatem BA, Abdullah WH, Hakimi MH, Mustapha KA (2016) Organic geochemistry characterization of Late Jurassic bituminous shales and their organofacies and oil generation potential in the Shabwah depression, southeast Sabatayn, Yemen. *Mar Pet Geol* 72:83–97
- Head L, Jones D, Larter S (2003) Biological activity in the deep subsurface and the origin of heavy oil. *Nature* 426:344–352
- Huang WY, Meinschein WG (1979) Sterols as ecological indicators. *Geochim Cosmochim Acta* 43:739–745
- Johns RB (1986) Biological markers in the sedimentary record. Elsevier, Amsterdam
- Killops SD, Funnell RH, Suggate RP, Sykes R, Peters KE, Walters C, Woolhouse AD, Weston RJ, Boudou JP (1998) Predicting generation and expulsion of paraffinic oil from vitrinite-rich coals. *Org Geochem* 29:1–21
- Larter S, Wilhelms A, Head I, Koopmans M, Aplin A, di Primio R, Zwach C, Erdmann M, Telnaes N (2003) The controls on the composition of biodegraded oils in the deep subsurface—part 1: biodegradation rates in petroleum reservoirs. *Org Geochem* 34:601–613
- Larter SR, Head IM, Huang H, Bennett B, Jones M, Aplin AC, Murray A, Erdmann M, Wilhelms A, di Primio R (2005) Biodegradation, gas destruction and methane generation in deep subsurface petroleum reservoirs: an overview. A.G. Dore, B. Vining (Eds.), *Petroleum Geology: Northwest Europe and Global Perspectives: Proceedings of the 6th Petroleum Geology Conference*, Geological Society, London 633–640
- Luo P, Gu Y (2005) Effects of asphaltene content and solvent concentration on heavy-oil viscosity. SPE/PS–CIM/CHOA international thermal operations and heavy oil symposium, Calgary (2005) 1–3. November. 1–7
- Luo P, Gu Y (2007) Effects of asphaltene content on the heavy oil viscosity at different temperatures. *Fuel* 86:1069–1078
- Mackenzie AS, Patience RL, Maxwell JR, Vandenbroucke M, Durand B (1980) Molecular parameters of maturation in the Toarcian shales, Paris Basin, France—I. Changes in the configurations of acyclic isoprenoid alkanes, steranes and triterpanes. *Geochim Cosmochim Acta* 44:1709–1721
- Makeen YM, Abdullah WH, Hakimi MH, Mustapha KA (2015) Source rock characteristics of the Lower Cretaceous Abu Gabra formation in the Muglad Basin, Sudan, and its relevance to oil generation studies. *Mar Petrol Geol* 59:505–516
- Moldowan JM, Sundaraman P, Schoell M (1985) Sensitivity of biomarker properties to depositional environment and/or source input in the Lower Toarcian of S.W. Germany *Org Geochem* 10:915–926
- Peters KE, Moldowan JM (1993) *The biomarker guide: interpreting molecular fossils in petroleum and ancient sediments: Englewood Cliffs*. Prentice Hall, New Jersey, p 363
- Peters KE, Walters CC, Moldowan JM (2005) *The biomarker guide*, 2nd edn. Cambridge University Press, Cambridge, p 1155
- Philp RP (1985) Biological markers in fossil fuel production. *Mass Spectrom Rev* 4:1–54
- Redfern P, Jones JA (1995) The interior rifts of Yemen—701 analysis of basin structure and stratigraphy in a regional plate tectonic context. *Basin Res* 7:337–356
- Roushdy MI, El Nady MM, Mostafa YM, El Gendy NS, Ali HR (2010) Biomarkers characteristics of crude oils from some oilfields in the Gulf of Suez. *Egypt J Am Sci* 6:911–925
- Sarki Yandoka BM, Abdullah WH, Abubakar MB, Hakimi MH, Mustapha KA, Adegoke AK (2015) Organic geochemical characteristics of Cretaceous Lamja formation from Yola Sub-basin, Northern Benue Trough, NE Nigeria: implication for hydrocarbon-generating potential and paleodepositional setting. *Arab J Geosci* 8:7371–7386
- Schwark L, Empt P (2006) Sterane biomarkers as indicators of Palaeozoic algal evolution and extinction events. *Palaeogeogr Palaeoclimatol Palaeoecol* 240:225–236
- Seifert WK, Moldowan JM (1978) Application of steranes, terpanes and monoaromatic to the maturation, migration and source of crude oils. *Geochim Cosmochim Acta* 42:77–95
- Seifert WK, Moldowan JM (1981) Paleo-reconstruction by biological markers. *Geochim Cosmochim Acta* 45:783–794
- Seifert WK, Moldowan JM (1986) Use of biological markers in petroleum exploration. In: RB Johns ed, 24, *Methods in Geochemistry and Geophysics Book*, Amsterdam Series (261–290)
- Sofer Z (1984) Stable carbon isotope compositions of crude oils: application to source depositional environments and petroleum alteration. *Am Assoc Pet Geol Bull* 68:31–49
- SPT (1994) *The Petroleum Geology of the Sedimentary Basins of the Republic of Yemen*. Unpublished Report V 1–7
- Summons RE, Thomas J, Maxwell JR, Boreham CJ (1992) Secular and environmental constraints on the occurrence of dinosterane in sediments. *Geochim Cosmochim Acta* 56:2437–2444
- Ten Haven HL, De Leeuw JW, Rullkötter J, Sinnighe Damsté JS (1987) Restricted utility of the pristane/phytane ratio as a palaeoenvironmental indicator. *Nature* 330:641–643
- Tissot B, Welte DH (1984) *Geochemical Fossils and Their Significance in Petroleum Formation*. Petroleum Formation and Occurrence. Springer, Berlin, pp 93–130
- Tserolas P, Maravelis AG, Tsochandarlis N, Pasadakis N, Zelilidis A (2019) Organic geochemistry of the Upper Miocene-Lower Pliocene sedimentary rocks in the Hellenic Fold and Thrust Belt, NW Corfu island, Ionian sea, NW Greece. *Mar Pet Geol* 106:17–29
- Wang W, Wang T, Li M, Mao F, Liu J, Xiao H, Lai H, Ai X (2021) The origins of biodegraded oils in sandstone reservoirs in the Termit Basin. *J Pet Sci Eng* 207:109130